

Ground-based Raman-lidar for day and night measurements of water vapor in the boundary layer

F. DE TOMASI, M. R. PERRONE and M. L. PROTOPAPA

*INFN, Istituto Nazionale di Fisica della Materia, Dipartimento di Fisica
Università di Lecce, Lecce, Italy*

(ricevuto il 9 Novembre 1999; revisionato il 4 Luglio 2000; approvato il 25 Luglio 2000)

Summary. — The solar-blind Raman-lidar based on a KrF laser (248 nm) developed at Lecce's University (40° 20' N, 18° 6' E) is described. The lidar is currently used for day and night measurements of water vapor. The dependence of the measurement range of the lidar on the laser beam divergence is investigated and it is shown that the KrF laser beam divergence can be reduced by a factor ~ 10 by using a quite simple unstable cavity configuration. The maximum range which was limited to approximately 500 m for a ~ 3 mrad divergence laser beam has increased up to 1200 m with a ~ 0.3 mrad divergence laser beam since the field of view of the telescope was of 1 mrad. Water vapor profiles retrieved from lidar measurements under different operating conditions are presented. The effect of boundary-layer ozone absorption has also been investigated.

PACS 96.20 – Meteorology.

1. – Introduction

Water vapor is one of the most important parameters of the atmosphere [1]. The spatial and temporal monitoring of water vapor concentration is crucial in order to understand a number of atmospheric processes: cloud formation, atmospheric circulation, hydrological cycle and energy transport within the atmosphere [2]. Radiosondes, passive satellite observations and lidars are currently used for measuring atmospheric water vapor. Radiosondes are quite expensive and may not provide a true vertical measurement. Observations from satellite provide broad geographic coverage but are limited in both accuracy and altitude resolution [1]. The Raman lidar and the DIAL (Differential Absorption Lidar) techniques are instead well established for measuring water vapor with good range resolution and continuously. The DIAL systems, though possessing higher sensitivity and a larger altitude range, are rather complicated and require a high level of stability for the laser wavelength as a consequence of the small bandwidth at the water absorption line [3]. Moreover, a DIAL system requires that the product of the number density, cross-section, and range element be greater than approximately 0.02, which restricts spatial resolution. So,

Raman lidar systems are chosen over DIAL systems because of their potential higher spatial resolution [4]. The Raman technique in the measurement of tropospheric water vapor was demonstrated in 1969 by Melfi *et al.* [5] and since then several Raman lidar have been developed and used all over the world. Note that an ultraviolet laser for which the Raman-scattered light remains in the solar-blind region of the spectrum (220–300 nm) is generally [1, 6] required for daylight operation of a Raman lidar. This restricts the wavelength of the laser to less than 270 nm and the maximum range of the lidar is severely reduced when it is used with UV laser sources as a consequence of atmospheric attenuation. However, daytime measurements of water vapor are of peculiar interest: many significant meteorological phenomena such as convective storm development occur more often during the day than at night [1]. Several studies have been conducted to optimize the operating wavelength of a solar-blind Raman lidar and it was found that the optimum wavelength is located between 260 and 262 nm: the figure of merit decreases because of atmospheric attenuation for smaller wavelengths and because of increasing solar background radiation for longer wavelengths [2, 7]. However, lidar systems based either on KrF (248 nm) excimer lasers [4, 8] or on Nd:YAG lasers [10] operating in a frequency-quadrupled mode (266 nm) have been developed for daytime measurements of water vapor. Quadrupled Nd-YAG and KrF lasers are the most reliable, commercial available radiation sources to realize solar blind Raman lidars. Note that maximum lidar ranges of about 1200 m have been reached with Raman lidar systems based on KrF and Nd:YAG lasers [10] operating in a frequency-quadrupled mode (266 nm).

This paper describes the Raman lidar system based on a KrF laser (248 nm) developed at Lecce University (UNILE, 40° 20' N, 18° 6' E). Lecce is a town located in the south of Italy and it is 20 km away from the Adriatic and the Ionian sea. The use of a KrF laser has been determined mainly by the laboratory availability. The UNILE lidar allows day and night measurements of water vapor and the effect of the KrF laser beam divergence on the maximum range of the lidar is investigated. A simple unstable cavity configuration has been introduced to significantly reduce the laser beam divergence. The method employed and the equipment are first described, then water vapor measurements conducted in Lecce under different operating conditions are presented.

2. – Methodology and experimental apparatus

As is well known, the water vapor mixing ratio r can be measured as a function of range z by means of the Raman lidar signal of water vapor, nitrogen and oxygen [10] with a solar-blind Raman lidar

$$(1) \quad r(z) = K[S_{\text{H}_2\text{O}}(z)/S_{\text{N}_2}(z)][S_{\text{O}_2}(z)/S_{\text{N}_2}(z)]^\gamma,$$

where K is a calibration factor, the factor with the oxygen Raman signal eliminates the effect of ozone absorption, and

$$(2) \quad \gamma = [\Delta\sigma(\text{H}_2\text{O}, \text{N}_2)]/[\Delta\sigma(\text{N}_2, \text{O}_2)],$$

where $\Delta\sigma(X, Y)$ is the ozone absorption cross-section difference for Raman wavelength λ_X and λ_Y . Note that eq. (1) is obtained by assuming that ozone is the only factor of wavelength-dependent attenuation [10] and that each Raman signal is

TABLE I. – Spectroscopic Raman data for an incident wavelength of 248 nm.

Species X	Raman shift (cm ⁻¹)	Scattered wavelength (nm)	Raman backscattering cross-section (m ² sr ⁻¹)
O ₂	1556	257.9	2.68 × 10 ⁻³³
N ₂	2330	263.7	1.30 × 10 ⁻³³
H ₂ O	3653	273.2	4.10 × 10 ⁻³³

given by

$$(3) \quad S_X(z) = k_X (d\sigma/d\Omega)_X (1/z^2) q(\lambda_0, z) q(\lambda_X, z) N_X,$$

where $(d\sigma/d\Omega)_X$ is the Raman backscattering cross-section for the species X, k_X is an instrumental factor, $q(\lambda, z)$ is the atmospheric transmission between ranges 0 and z , N_X is the concentration of the species X, and λ_0 is the laser wavelength. The main spectroscopic Raman data for an incident wavelength of 248 nm taken from the literature are reported in table I.

The experimental set-up of the lidar system which utilizes a KrF laser (Lambda Physik LPX 210 i) as radiation source is at first described. Commercial excimer lasers are mainly fitted with a plane parallel cavity. The KrF laser, equipped with a conventional plane-parallel cavity (fig. 1a) made of a dielectric coated flat mirror M_1 as full reflector and a flat quartz as output coupler (M_2), produces laser pulses of 650 mJ energy and of 35 ns duration at a maximum repetition rate of 100 Hz. Moreover, the laser output beam has a cross-section of 12×23 mm² and a divergence of 1.5×4.0 mrad.

Unstable cavities may be applied to excimer lasers to reduce their beam divergence,

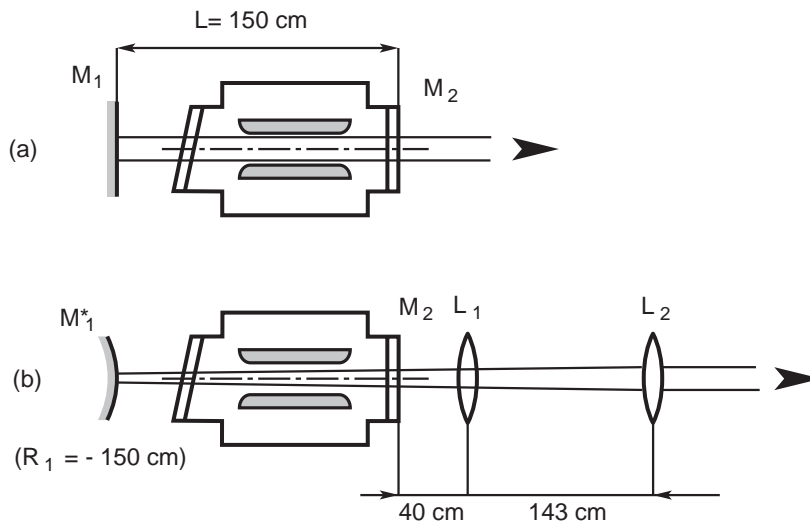


Fig. 1. – Plane-parallel cavity configuration (a), unstable cavity configuration and collimating lenses L_1 and L_2 (b).

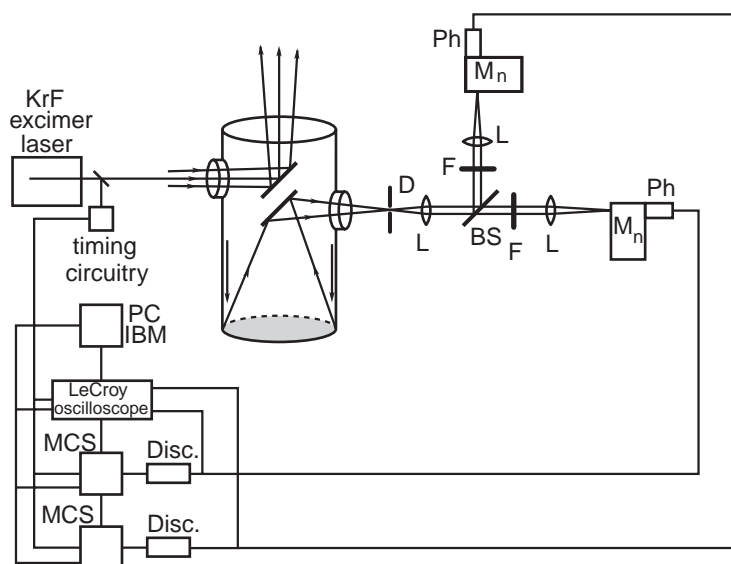


Fig. 2. – Schematic set-up of the lidar system; D: diaphragm; L: lenses; BS: beam splitter; F: neutral density filters; Mn: monochromator; Ph: photosensor.

as is well known [11]. Then, a nonconfocal unstable cavity of magnification factor $M = 5.8$ has been applied to the KrF laser. The cavity was easily realized by replacing the rear flat mirror with a dielectric coated convex mirror (M_1^*) having radius of curvature $R = -150$ cm (fig. 1b). It has been found that the KrF laser fitted with the unstable cavity generates pulses of 600 mJ energy, 35 ns duration and with a divergence of 0.2×0.4 mrad. Two lenses L_1 and L_2 of 10 and 5 m focal length respectively, set 143 cm apart, have been used to get a collimated output beam with a cross-section of 20×30 mm².

Figure 2 shows the set-up of the main lidar components. Collection of the backscattered radiation is obtained by a Newtonian telescope whose primary mirror has 30 cm diameter and 120 cm focal length. A 1.2 mm field stop aperture (D) located on the telescope focus limits its field of view to approximately 1 mrad. The collected radiation is divided by a 50% beam splitter (BS) into two channels. A double-grating monochromator (Jobin-Yvon DH10 UV) characterized by an out-of-band rejection better than 10^{-7} and a spectral resolution of 0.4 nm when used with a 0.5×8 mm² central slit, is used in each Raman channel to spectrally resolve the backscattered radiation. No cross talk between nearby lines has been observed. Note that each monochromator grating is characterized by a relative efficiency of about 15% in the spectral range of interest and as a consequence the sensitivity of both detection channels is relatively low. Each Raman signal is detected in the photon-counting regime by a photosensor module (Hamamatsu H5783p-06) connected to a 300 MHz discriminator (Phillips Scientific Mod. 6908) and a multichannel scaler (EG&G MCS-Mod. 914 P). The photosensor modules including a compact photomultiplier tube and a built-in high-voltage power supply, are characterized by a gain of 1.27×10^6 at the control voltage of 0.8 V, by a fast time response (0.65 ns) and a low dark current (0.06 nA) and dark count (11 s⁻¹). Neutral density filters (F) in front of the

monochromator are only required for N_2 and O_2 Raman signal measurements to reduce count rates. The multichannel scaler operates with a dwell time of 100 ns, yielding a spatial resolution of 15 m, even if its minimum dwell time is 5 ns. The system is fully remote controlled by a home-developed software.

3. – Measurements

All measurements presented in this paper have been recorded by sending in the atmosphere laser pulses of 50 mJ energy, 35 ns duration at a repetition rate of 50 Hz. Note that the lidar system UNILE has only two Raman channels and as a consequence O_2 and N_2 signals are first measured to evaluate the effect of the boundary-layer ozone absorption according to eq. (1). Then, H_2O and N_2 signals are measured. The ozone absorption profile is assumed not to change throughout the day hours when water vapor measurements are taken [2]. Indeed, the ratio $S_{O_2}(z)/S_{N_2}(z)$ has not been observed to vary significantly with time of day or with time over the course of few days. These results may be due to the fact that measurements have been taken in a rural area. So we believe that the assumption of constant ozone profile throughout the day hours is not a bad one when water vapor measurements are taken in nonpopulated areas, according to ref. [4].

Raman lidar measurements taken with the KrF laser fitted with the plane-parallel cavity are at first presented. Figure 3 shows typical photon count signals for nitrogen (dotted line) and oxygen (solid line) Raman channel, both obtained by averaging signals over about half-hour time (corresponding to 100.000 laser shots) with a vertical resolution of 15 m. The measurements started at 1100 (LST) on June 10, 1999. That day was characterized by clear-sky conditions. Different filters have been used in both channels to keep the peak count rate below the value at which corrections for pulse pileup would be required [6]. Both Raman signals increase from zero at the surface to a peak value near 50 m altitude as the laser beam moves fully into the field of view (FOV) of the telescope. For a perfectly designed and aligned optical system the beam overlap

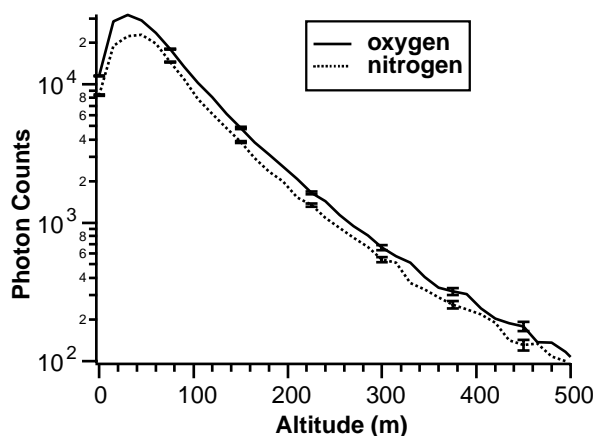


Fig. 3. – Photon counts *vs.* altitude accumulated on June 10, 1999 during half an hour data acquisition period (10^5 laser shots) on oxygen (solid line) and nitrogen (dotted line) Raman channel. Error bars indicate the $1 - \sigma$ uncertainty of the lidar measurements calculated by assuming Poisson statistics.

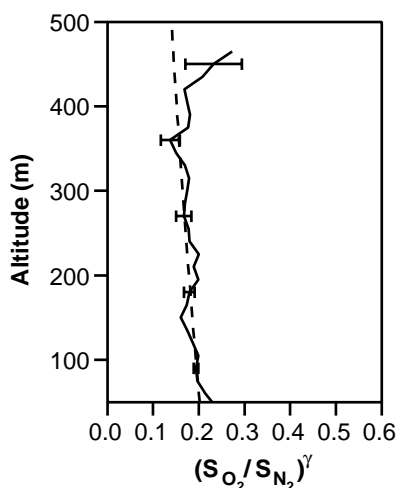


Fig. 4. – Ozone transmittivity profile up to a multiplicative factor (solid line), recorded at 1100 (LST) on June 10, 1999. The ozone transmittivity (---) calculated for a constant ozone concentration ($\langle O_3 \rangle = 2.5 \times 10^{18} \text{ m}^{-3}$) up to a multiplicative factor is shown for comparison.

factor should be similar for both oxygen and nitrogen signals, it will tend to cancel in the ratio and as a consequence measurements could also be retrieved below the height of complete overlap laser-beam receiver-FOV [1]. If, however, the overlap function is not the same for the two signals a system calibration function must be applied to the data [5]. Figure 4 displays the $[S_{O_2}(z)/S_{N_2}(z)]^\gamma$ factor, where the $S_{O_2}(z)/S_{N_2}(z)$ ratios have been multiplied by the experimentally determined range-dependent calibration function to remove differences between the beam overlap factor of both channels. We have determined the calibration function by tuning both detection channels on the nitrogen Raman wavelength and by recording measurements in this configuration, according to [5,6]. The data shown in fig. 4 have been smoothed using a running average of three data points resulting in an overall altitude resolution of 45 m. The error bars represent the $1\text{-}\sigma$ uncertainty of the lidar measurements calculated by assuming Poisson statistics for the photon counts [6]. The uncertainty due to variations of atmospheric optical properties during signal acquisition has been neglected. Noise due to photomultiplier dark current and sky background light has not been observed for all measurements.

Figure 5 displays some water vapor profiles recorded at Lecce on June 10, 1999 at different hours of the day. We have used *in situ* measurements taken at an altitude of 30 m to determine the calibration factor K in (1). Indeed, the water vapor profile taken at ~ 1200 (LST) which is characterized by a smooth variation in the lower layer has been used to determine the K value by comparison with *in situ* measurements, in order to reduce errors due to the larger value of the lidar minimum altitude. Note that the water vapor and nitrogen channel ratios have also been corrected for the range-dependent calibration ratios due to differences between the two channels. Figures 4 and 5 reveal that the maximum effective range of the lidar is approximately 500 m for a ~ 3 mrad divergence KrF laser beam, according to refs. [4,9]. All profiles are rather homogeneous as a consequence of the convective activity of a day

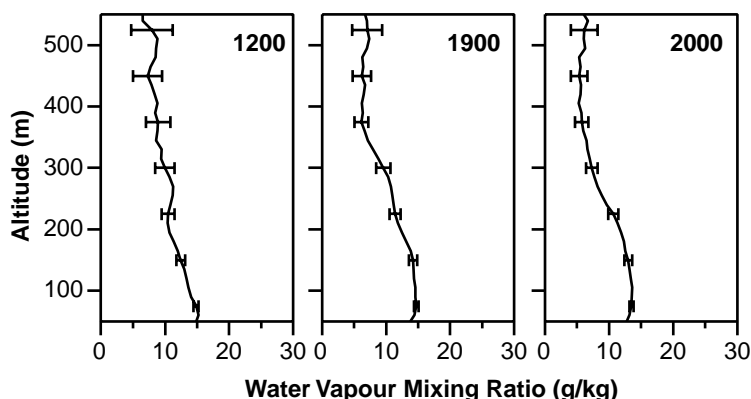


Fig. 5. – Water vapor mixing ratio profiles recorded at different hours of the day (LST) on June 10, 1999 by averaging 10^5 laser shots. Error bars indicate the $1-\sigma$ uncertainty of the lidar measurements calculated by assuming Poisson statistics. The data have been smoothed with an average window length of 45 m.

characterized by clear-sky conditions and the water vapor mixing ratio decreases from 13.5–14.5 g/kg at 100 m to approximately 8 g/kg at 500 m. Note that the mixing ratio decreases faster with altitude at the sunset (fig. 5) because of the lowering [12] of the planetary boundary layer (PBL) and reaches a value of ~ 8 g/kg at 300 m at 2000 (LST).

Some profiles of the $[S_{O_2}(z)/S_{N_2}(z)]^\gamma$ factor and of the water vapor mixing ratio retrieved with the ~ 0.3 mrad divergence KrF laser beam are shown in figs. 6 and 7,

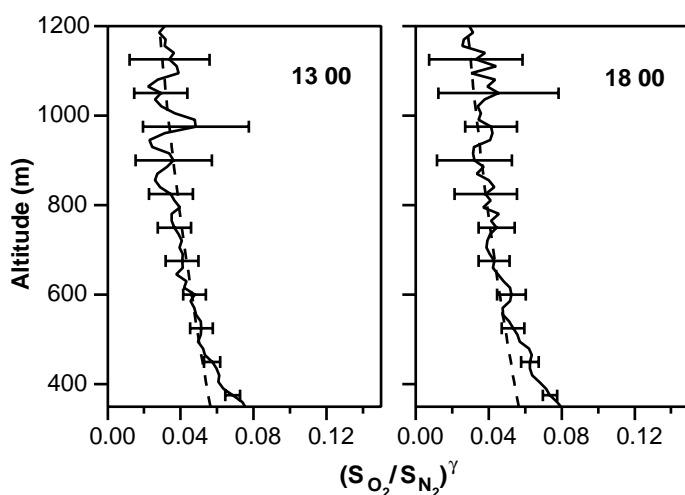


Fig. 6. – Ozone transmittivity profiles up to a multiplicative factor recorded at different hours of the day (LST) on July 15, 1999 by averaging 50 000 laser shots. Error bars indicate the $1-\sigma$ uncertainty of the lidar measurements calculated by assuming Poisson statistics. The ozone transmittivity (---) calculated for a constant ozone concentration ($\langle O_3 \rangle = 2.5 \times 10^{18} \text{ m}^{-3}$) up to a factor is shown for comparison.

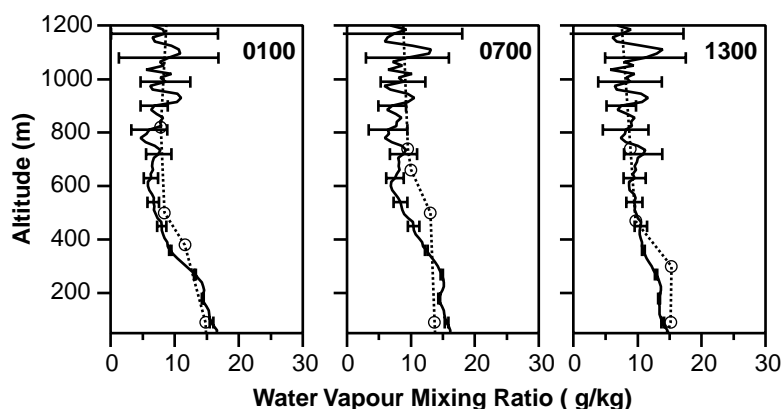


Fig. 7. – Water vapor mixing ratio profiles recorded at different hours of the day (LST) on July 28, 1999 by averaging 10^5 laser shots. Error bars indicate the $1\text{-}\sigma$ uncertainty of the lidar measurements calculated by assuming Poisson statistics. The data have been smoothed with an average window length of 45 m.

respectively. Figure 6 displays the $[S_{O_2}(z)/S_{N_2}(z)]^y$ factor measured at different hours of the day on July, 15 1999. The measurements have been obtained by averaging 50000 laser shots and the procedure outlined above has been followed to retrieve both profiles. One observes that the effect of boundary-layer ozone absorption does not vary significantly with time of the day, at least within our experimental errors. Figure 6 also reveals that the ozone concentration does not change significantly with altitude at least up to the maximum range of our lidar system. In fact, the dotted line in fig. 6 represents the ozone transmittivity *vs.* altitude calculated up to a multiplicative factor for a constant ozone concentration $\langle O_3 \rangle = 2.5 \times 10^{18} \text{ m}^{-3}$ [13]. A fair accordance between experimental and analytical curves turns out from fig. 6. It is believed that we have not observed large variations of the ozone transmittivity profile with time since the UNILE-lidar is in a rural area far away from polluting anthropic activities. Significant evolution of the ozone concentration with time of the day and or with time over the course of few days is expected as a consequence of the photochemical air pollution typical of many big cities [14]. Note that the dotted line in fig. 4 also represents the ozone transmittivity up to a multiplicative factor for a constant ozone concentration of $2.5 \times 10^{18} \text{ m}^{-3}$.

Some water vapor mixing ratio profiles retrieved from measurements recorded on July 28, 1999 by averaging 10^5 laser shots are shown in fig. 7. The procedure previously outlined has been followed to retrieve these profiles. One observes that the maximum effective range of the lidar is approximately 1200 m under the latter experimental conditions. *In situ* measurements taken at an altitude of 30 m have been used to determine the calibration factor K in (1).

The profiles of fig. 7 are representative of the water vapor mixing ratio time evolution in clear-sky conditions. One observes that the mixing ratio reaches a minimum value of $\sim 6.5 \text{ g/kg}$ at an altitude of 500 m at 0100 (LST) and at $\sim 600 \text{ m}$ at 0700 (LST). A slower decrease of the mixing ratio with altitude is observed at 1300 (LST). Indeed, an almost height-constant water vapor mixing ratio is measured at 1300 as a consequence of a strong turbulent mixing from the ground up to 1200 m (fig. 7b). These

profiles (fig. 7) are also representative of the diurnal cycle of the PBL height which is expected to reduce to about 400 m at nights in narrow lands between two seas and to be fully developed at 1400 hours [12].

A comparison of water vapor mixing ratio profiles measured with the lidar at Lecce and with a balloon sonde at Brindisi (40° 39' N, 15° 57' E) located near the Adriatic sea, about 35 km northeast of Lecce, is also shown in fig. 7. Balloon sonde measurements at the lidar site were not available. In view of the spatial separation of the two experiments, the agreement is good. Moreover, the comparison shown in fig. 7 gives confidence in the lidar calibration and measurements. It is worth mentioning that the depth of the PBL over the sea is expected to be almost uniform in space and in time, whereas, over the land, the PBL structure shows a great variability which is strongly correlated to the solar zenith angle and to the orography of the area of interest [15].

4. – Conclusion

A solar-blind Raman lidar based on a KrF laser (248 nm) has been developed at Lecce University (40° 20' N, 18° 6' E) and has been used for retrieving diurnal and nocturnal measurements of water vapor mixing ratio profiles at least up to 1.2 km. These measurements are of peculiar interest to evaluate the vertical structure of the PBL. A great variability of the PBL is expected in Lecce which is quite close (~ 20 km) to the Adriatic and Ionian sea, respectively.

It has been shown how the measurement range of the lidar increases with laser beam divergence. Indeed, it has been shown that the beam divergence of commercially available KrF lasers, which are generally delivered with a plane-parallel cavity, can be reduced by a factor of ~ 10 by replacing the flat full-reflector mirror of the laser cavity with a full-reflector convex mirror, in order to realize an unstable cavity. A maximum lidar range of about 1200 m has been reached with a 50 mJ energy KrF laser beam of low divergence (~ 0.3 mrad) and a 30 cm diameter telescope by averaging 10^5 laser shots, despite the high losses of both detection Raman channels. It is worth mentioning that most of the water vapor content is in the PBL and that significative spatial and temporal evolutions of the water vapor mixing ratio are mainly expected to occur within the first few kilometers from the ground.

Finally, it has been shown that the ratio $S_{O_2}(z)/S_{N_2}(z)$ and then the effect of boundary-layer ozone absorption do not vary significantly with time of the day and this result has been ascribed to the fact that measurements have been taken in a nonpopulated area. As a consequence, a two-channel Raman lidar has been used to retrieve time evolution of water vapor mixing ratio profiles.

Work is in progress to further improve the KrF laser beam divergence by increasing the magnification factor of the unstable cavity and test the benefits on the maximum range of the lidar system. A further increase of the lidar range is also expected to be reached by using in both Raman channels interference filters instead of monochromators, for the lower losses of interference filters.

* * *

This work has been partially supported by “Provincia di Lecce”. FdT holds a EU Marie Curie fellowship. We gratefully acknowledge scientific suggestions for the lidar realization of prof. N. SPINELLI and dr. G. PAPPALARDO and discussions on measurements with dr. P. MARTANO. The Istituto per l’Inquinamento Atmosferico e

l'Agronometria (ISIAtA) of the Consiglio Nazionale delle Ricerche (CNR) is gratefully acknowledged for providing the *in situ* meteorological data. The Aeronautica Militare, Comando Aeroporto di Brindisi is gratefully acknowledged for providing the radiosonde measurements.

REFERENCES

- [1] MELFI S. H. and WHITEMAN D., *Observation of lower-atmospheric moisture structure and its evolution using a Raman lidar*, *Bull. Am. Meteorol. Soc.*, **66** (1985) 1288-1292.
- [2] RENAUT D. and CAPITINI R., *Boundary-layer water-vapor probing with a solar-blind Raman lidar: validations, meteorological observations and prospects*, *J. Atm. Oceanic Technol.*, **5** (1988) 585-600.
- [3] KIM D., CHA H., PARK J., LEE J. and VESELOVSKII I., *Daytime Raman lidar for water vapor and ozone concentration measurements*, *J. Korean Phys. Soc.*, **30** (1997) 458-462.
- [4] EICHINGER W. E., COOPER D. I., ARCHULETTA F. L., HOF D., HOLTKAMP D. B., KARL R. R. jr., QUICK C. R. and TIEE J., *Development of a scanning, solar-blind, water Raman lidar*, *Appl. Optics*, **33** (1994) 3923-3932.
- [5] WHITEMAN D. N., MELFI S. H. and FERRARE R. A., *Raman lidar system for the measurement of water and aerosol in the Earth's atmosphere*, *Appl. Optics*, **31** (1992) 3068-3082.
- [6] GOLDSMITH J. E. M., BLAIR F. H., BISSON S. E. and TURNER D. D., *Turn-key Raman lidar for profiling atmospheric water vapor, clouds, and aerosol*, *Appl. Optics*, **37** (1998) 4979-4990.
- [7] PETRI K., SALIK A. and COONEY J., *Variable-wavelength solar-blind Raman lidar for remote measurement of atmospheric water vapor concentration and temperature*, *Appl. Optics*, **21** (1982) 1212-1218.
- [8] COONEY J., PETRI K. and SALIK A., *Measurements of high resolution atmospheric water vapor profiles by use of a solar blind Raman lidar*, *Appl. Optics*, **24** (1985) 104-108.
- [9] EICHINGER W. E., COOPER D. I., PARLANGE M. and KATUL G., *The application of a scanning water Raman-lidar as a probe of atmospheric boundary layer*, *IEEE Transact. Geosci. Rem. Sensing*, **31** (1993) 70-79.
- [10] RENAUT D., POURNY J. C. and CAPITINI R., *Daytime Raman-lidar measurements of water vapor*, *Optics Lett.*, **5** (1980) 233-235.
- [11] C. GIURI, M. R. PERRONE and V. PICCINNO, *Output coupler design of unstable cavities for excimer lasers*, *Appl. Optics*, **36** (1997) 1143-1148.
- [12] BELLECCI C., DALU G. A., AVERSA P., CASELLA L., FEDERICO S. and P. GAUDIO P., *Evolution of water vapor profiles over complex terrain: observation and comparison with model simulations in the valley of Cosenza*, *Proceedings of the Europto Conference, Florence 20-24 September, 1999*, *Spie vol. 3865* (2000) 108.
- [13] BROWELL E. V., ISMAIL S. and SHIPLEY S. T., *Ultraviolet DIAL measurements of O₃ profiles in regions of spatially inhomogeneous aerosol*, *Appl. Opt.*, **24** (1985) 2827-2836.
- [14] DURIEUX E., FIORANI L., CALPINI B., FLAMM M., JAQUET L. and VAN DEN BERG H., *Tropospheric ozone measurements over the great Athens area during the MEDCAPHOT-trace campaign with a new shot-per-shot DIAL instrument: experimental system and results*, *Atmosph. Environment*, **32** (1998) 2141-2150.
- [15] SANTACESARIA V., MARENCO F., BALIS D., PAPAYANNIS A. and ZEREFOS C., *Lidar observations of the planetary Boundary Layer above the city of Thessaloniki, Greece*, *Nuovo Cimento*, **21** (1998) 585-596.